An angular cutoff composite model for investigation on electromagnetic scattering from two-dimensional rough sea surfaces*

Nie Ding(聂 丁) and Zhang Min(张 民)†

School of Science, Xidian University, Xi'an 710071, *China*

(Received 24 October 2009; revised manuscript received 3 February 2010)

Based on the local configuration angle division to select the corresponding method for electromagnetic scattering calculation from rough sea surface, this paper presents an angular cutoff composite model: when the local scattered angle is in the specular region that is given by an approximately 20 degrees cone around the specular direction, the Kirchhoff approximation is applied to evaluate the specular reflection, which dominates the total scattering in this region; the small perturbation method is employed to handle the diffuse reflection which is predominant as the local scattered angle is situated out of the specular region. Numerical results are compared with those of experimental and theoretical models in several configurations as a function of incident angle, wind speed, wind direction. The comparison of numerical results of other experimental and theoretical models in several configurations shows that the new composite model is robust to give accurate numerical evaluations for the sea surface scattering.

Keywords: electromagnetic scattering, composite surface model, rough sea surface, angular cutoff
PACC: 4110H, 5235H

1. Introduction

In recent years, the study of electromagnetic scattering from the sea surface has obtained more and more attention in many fields, such as environmental monitoring, target detection and recognition, radiowave propagation and communication, etc.[1–5] Several methods[6,7] have been published that can theoretically cope with the sea-surface scattering, some among them are the Kirchhoff approximation (KA), the small perturbation method (SPM), the phase perturbation method,[8] the two-scale model (TSM)[9] and the small slope approximation (SSA).[10]

As we have known, the KA works well in the near-specular directions and the SPM is appropriated to apply when the scattering is situated between specular and grazing angles. In a word, KA and SPM both have good performances in their specified angular ranges. Based on the idea of taking advantage of the KA and SPM without dwelling on the tough question about choosing the proper cutoff parameter like TSM, an angular cutoff composite model (ACCM) is proposed. In this paper, the electromagnetic scattering from two-dimensional sea surface is investigated by the ACCM. Numerical results of the scattering are presented, compared and discussed in detail.

2. Formulation

First of all, an explanation of the specular region for this new model is illustrated in Fig. 1, it is approximately a cone of 20° semi-cone angle around the specular direction.

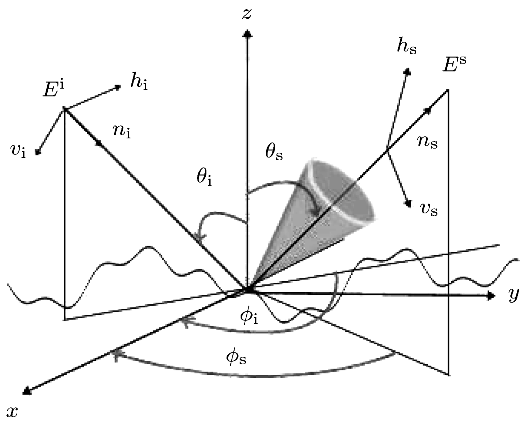

Fig. 1. Geometry of the surface-scattering problem.

Based on the consideration that KA should only be valid when near the specular direction (±20°), the

*Project supported by the National Natural Science Foundation of China (Grant No. 60871070), the National Pre-research Foundation and the Foundation of the National Electromagnetic Scattering Laboratory.

†Corresponding author. E-mail: mzhang@mail.xidian.edu.cn

http://www.iop.org/journals/cpb http://cpb.iphy.ac.cn

cutoff angle of 20° is thus chosen. The similar conclusion can be found in Ref. [11]. If $\theta_\mathrm{s} = \theta_\mathrm{i}$, $\phi_\mathrm{s} = \phi_\mathrm{i}$ holds in Fig.1, the cone plotted in the figure is the very specular region for the forward–backward bistatic scattering configuration.

When it comes into the case that the local scattered angle is in the specular region, KA is applied to evaluate the specular reflection, which dominates the total scattering in this region. The KA with the simplification of the stationary-phase approximation is adequate to give a more accurate result; the SPM is employed to deal with the diffuse reflection reigned by small roughness as the local scattered angle is situated out of the specular region.

Let $z(x,\ y)$ represent the rough height of the sea surface and Z_x, Z_y are its derivatives along the x-axis and y-axis directions respectively. Let the unprimed coordinates be the reference frame and let the primed coordinates be the local frame. The unit normal vector to $z(x,\ y)$ can be written in terms of $Z_x,\ Z_y$ as follows:

$$\hat{\boldsymbol{n}} = (-\hat{\boldsymbol{x}}Z_x - \hat{\boldsymbol{y}}Z_y + \hat{\boldsymbol{z}})/\sqrt{1+Z_x^2+Z_y^2}. \tag{1}$$

Let the incident plane wave lie in the xz-plane, see Fig. 1, we have $\phi_\mathrm{i} = 0$, its direction of propagation equals

$$\hat{\boldsymbol{n}}_\mathrm{i} = \hat{\boldsymbol{x}}\sin\theta_\mathrm{i}\cos\phi_\mathrm{i} + \hat{\boldsymbol{y}}\sin\theta_\mathrm{i}\sin\phi_\mathrm{i} - \hat{\boldsymbol{z}}\cos\theta_\mathrm{i}. \tag{2}$$

Its counterpart of the scattered wave equals

$$\hat{\boldsymbol{n}}_\mathrm{s} = \hat{\boldsymbol{x}}\sin\theta_\mathrm{s}\cos\phi_\mathrm{s} + \hat{\boldsymbol{y}}\sin\theta_\mathrm{s}\sin\phi_\mathrm{s} + \hat{\boldsymbol{z}}\cos\theta_\mathrm{s}. \tag{3}$$

The local unit coordinate vectors are defined as follows:

$$\hat{\boldsymbol{z}}' = \hat{\boldsymbol{n}}, \tag{4}$$

$$\hat{\boldsymbol{y}}' = \frac{(\hat{\boldsymbol{n}} \times \hat{\boldsymbol{n}}_\mathrm{i})}{|\hat{\boldsymbol{n}} \times \hat{\boldsymbol{n}}_\mathrm{i}|}, \tag{5}$$

$$\hat{\boldsymbol{x}}' = \hat{\boldsymbol{y}}' \times \hat{\boldsymbol{z}}'. \tag{6}$$

After using the stationary-phase approximation to simplify the corresponding scattered field expression, the final polarized scattering coefficient developed by KA is expressed as

$$\sigma_{rt,\mathrm{KA}} = \frac{\pi k^2 \left|\boldsymbol{q}\right|^2}{q_z^4} \left|U_{rt}\right|^2 \mathrm{Prob}(Z_x, Z_y), \tag{7}$$

where $r,\ t$ = H or V, H indicates horizontal polarization (HH-pol), V vertical polarization (VV-pol). $\boldsymbol{q} = k(\hat{\boldsymbol{n}}_\mathrm{s} - \hat{\boldsymbol{n}}_\mathrm{i}) = [q_x, q_y, q_z]$, $Z_x = -q_x/q_z$, $Z_y = -q_y/q_z$. The U_{rt} is a polarimetric parameter depending on the configuration angles $(\theta_\mathrm{i}, \phi_\mathrm{i}, \theta_\mathrm{s}, \phi_\mathrm{s})$ and on Fresnel coefficients;[12] $\mathrm{Prob}(Z_x, Z_y)$ is the probability density function of the surface slopes.[13] The validity condition for the KA under stationary-phase approximation can be written as

$$k\sigma > \frac{\sqrt{10}}{|\cos\theta_\mathrm{s} + \cos\theta_\mathrm{i}|} \quad kl > 6 \quad \text{and} \quad R_\mathrm{c} > \lambda, \tag{8}$$

here σ is the surface standard deviation, l is the surface correlation length and R_c is the average radius of curvature for the rough surface.

The scattering coefficient developed by SPM is formulated as follows:

$$\sigma_{rt,\mathrm{SPM}} = 8k^4\cos^2(\theta_\mathrm{i})\cos^2(\theta_\mathrm{s})\left|\alpha_{rt}\right|^2 S(\left|\boldsymbol{K}_1\right|, \phi) \tag{9}$$

with

$$\boldsymbol{K}_1 = \begin{bmatrix} k\sin(\theta_\mathrm{s})\cos(\phi_\mathrm{s}-\phi_\mathrm{i}) - k\sin(\theta_\mathrm{i}) \\ k\sin(\theta_\mathrm{s})\sin(\phi_\mathrm{s}-\phi_\mathrm{i}) \end{bmatrix}, \tag{10}$$

α_{rt} is polarimetric coefficient expressed as

$$\alpha_\mathrm{HH} = -\frac{(\varepsilon_r - 1)\cos\phi_\mathrm{s}}{[\cos\theta_\mathrm{i} + (\varepsilon_r - \sin^2\theta_\mathrm{i})^{1/2}][\cos\theta_\mathrm{s} + (\varepsilon_r - \sin^2\theta_\mathrm{s})^{1/2}]}, \tag{11}$$

$$\alpha_\mathrm{VV} = \frac{(\varepsilon_r - 1)[\varepsilon_r\sin\theta_\mathrm{i}\sin\theta_\mathrm{s} - \cos\phi_\mathrm{s}(\varepsilon_r - \sin^2\theta_\mathrm{i})^{1/2}(\varepsilon_r - \sin^2\theta_\mathrm{s})^{1/2}]}{[\varepsilon_r\cos\theta_\mathrm{i} + (\varepsilon_r - \sin^2\theta_\mathrm{i})^{1/2}][\varepsilon_r\cos\theta_\mathrm{s} + (\varepsilon_r - \sin^2\theta_\mathrm{s})^{1/2}]}, \tag{12}$$

where $S(k,\phi) = S(k)f(k,\phi)$, $S(k,\phi)$ denotes two-dimensional sea spectrum,[14] which is applied to simulate sea surface. The validity condition is expressed as

$$k\sigma < 0.3, \quad k\sigma < \frac{0.3}{\sqrt{2}}kl. \tag{13}$$

Finally, a backscattering-coefficient expression using ACCM is given by

$$\sigma_{rt,\mathrm{ACCM}} = \begin{cases} <\sigma_{rt,\mathrm{KA}}(\theta_\mathrm{i}', \phi_\mathrm{i}', \theta_\mathrm{s}', \phi_\mathrm{s}')>, & \arccos\theta_\mathrm{s}' < 20^\circ, \\ <\sigma_{rt,\mathrm{SPM}}(\theta_\mathrm{i}', \phi_\mathrm{i}', \theta_\mathrm{s}', \phi_\mathrm{s}')>, & \text{otherwise}, \end{cases} \tag{14}$$

where $(\theta_i', \phi_i', \theta_s', \phi_s')$ are local configuration angles,[15] the symbol $\langle\ \rangle$ in Eq. (14) denotes an assemble average which can be calculated as

$$\langle\sigma\rangle = \frac{1}{M}\frac{1}{N}\sum_{m=1}^{M}\sum_{n=1}^{N}\sigma\left(Z_x(x_m, y_n), Z_y(x_m, y_n)\right), \quad (15)$$

where M and N are the number of the points discretized at equal interval along the x-axis and y-axis directions, $Z_x(x_m, y_n)$ and $Z_y(x_m, y_n)$ are the discretized forms of the $Z_x(x, y)$ and $Z_y(x, y)$.

The expression for the bistatic scattering coefficient has the same form with that of backscattering, except for the expression for the corresponding specular region. For the sake of brevity, we safely omit it.

3. Numerical results and discussion

In all the following numerations, except for the special declaration, the incident electromagnetic frequency f is 14.0 GHz, the permittivity of the sea water is 32.349644+36.615556i, u is the wind speed at an altitude of 10 m above the sea surface.

First, a two-dimensional rough sea surface of 50×50 discretized points at equal interval (1 m) is simulated as an example. Table 1 shows the number of the points handled by each component model (KA or SPM) of ACCM as the configuration angles around 20°. When the scattered angle in reference coordinates is less than 20°, in the specular region for backscattering configuration, the number of surface points should handled by the KA, which is far more than its counterpart of the SPM. The contrary phenomenon can be observed when the scattered angle is much greater than 20°. When the scattered angle equals 20°, the numbers of the points calculated by either model almost have equal shares in all 2500 points. It is the local configuration angle we used as an indicator, not the angle in reference coordinates. In addition, as seen in Eq. (15), the final scattering coefficient for each single configuration angle should be an assemble average of the coefficients of $M \times N$ points of the rough sea surface.

Table 1. The number of the points handled by KA or SPM in all 2500 discretized points.

model	16°	17°	18°	19°	20°	21°	22°	23°	24°
KA	2103	1906	1705	1426	1128	838	593	376	243
SPM	397	594	795	1074	1372	1662	1907	2124	2257

Both the above aspects ensure the smooth transition between the KA and SPM in the ACCM, which can be seen in Fig. 2. The relationship between the ACCM and its component models (KA and SPM) is illustrated in Fig. 2.

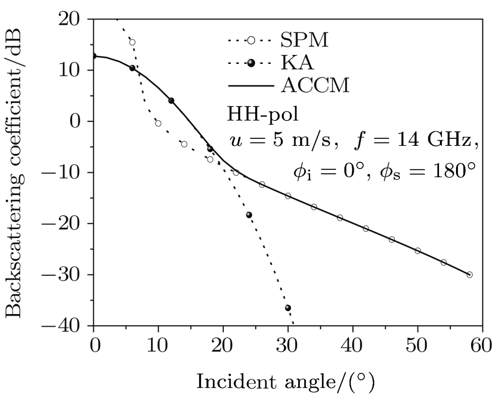

Fig. 2. Comparison between ACCM and its component models (KA and SPM) for backscattering coefficient from rough sea surface.

Figure 3 illustrates the comparison between ACCM and the Seasat Scatterometer II (SASS-II) model data[16,17] for the angular distribution of backscattering coefficient from rough sea surface with different wind speeds (5 m/s, 10 m/s) for HH-pol and VV-pol. The overall good match is obtained for HH-pol. The agreement between ACCM and the experimental data is good in the small incident angle region. In the region near cutoff angle (20°), the agreement is a little weak. This may be explained by the fact that the change of the surface slope at the cutoff angle between the two component models is a little discontiguous, nevertheless the final curve in the transition region is much smooth. While in large incident angle region, the VV-polarized backscattering coefficient is a little higher than the experimental data. This phenomenon is probably due to the fact that the sea surfaces simulated are stochastic in statistics, hence the scattering from such sea surfaces is also random, even after an assemble average. Thereby, to some extent, there may be an acceptable discrepancy between the corresponding scattering results and the SASS-II model.

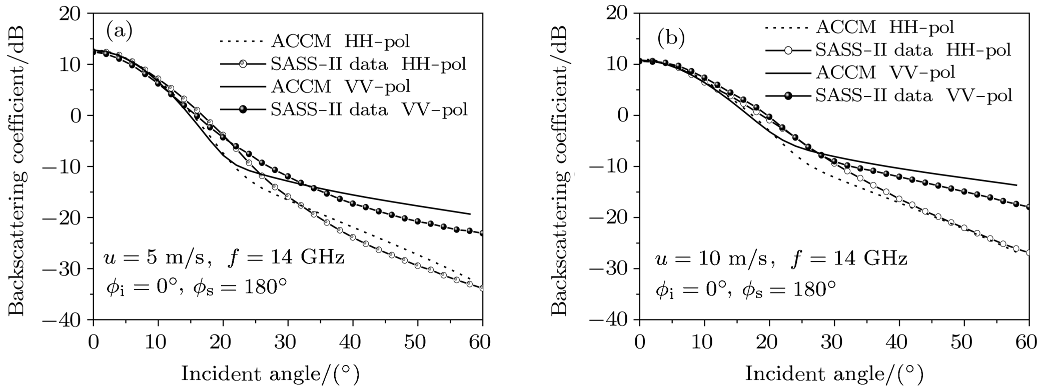

Fig. 3. Comparison between ACCM and the SASS-II model data for the angular distribution of backscattering coefficient from rough sea surface: (a) $u = 5$ m/s; (b) $u = 10$ m/s.

Figure 4 illustrates the dependence of the angular distribution of the backscattering coefficient given by the ACCM on the wind direction. Two different forms of angular distribution of the backscattering characteristics are presented. Figure 4(a) shows the value of the backscattering coefficients for VV-pol with fixed ϕ_i and ϕ_s by letting θ_i (or θ_s) vary. While in Fig. 4(b), with a constant incident angle $\theta_i = 30°$, comparison of the backscattering coefficient for HH-pol with varying ϕ_i between the ACCM and the RADSCAT experimental measured data[18] is presented, where 0° and 180° denote the upwind direction and downwind direction, respectively, 90° represents the crosswind direction. The difference between the upwind and crosswind is well illustrated, in addition, the discrepancy between the ACCM result and the experimental data is in normal and acceptable range.[11]

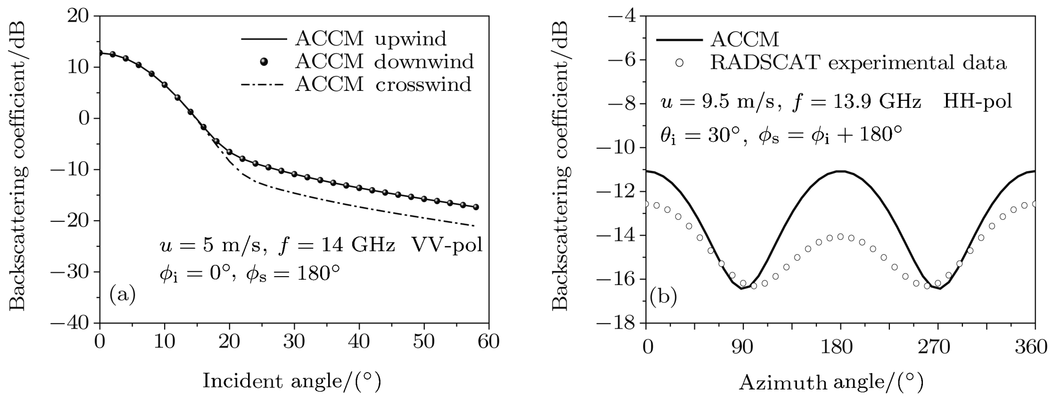

Fig. 4. The dependence of the angular distribution of the backscattering coefficient on the wind direction: (a) VV-pol, $u = 5$ m/s, $f = 14$ GHz; (b) HH-pol, $\theta_i = 30°$, $u = 9.5$ m/s, $f = 13.9$ GHz.

The forward-backward configuration is a particular case of the bistatic configuration. In Fig. 5, the angular distribution of the scattering coefficient for different wind speeds in the forward-backward configuration is depicted. Let $\phi_i = 0°$, $\phi_s = 0°$, θ_s vary from $-90°$ to 90°, see Fig. 1. It is clearly that the peak is located around the specular direction, which is a logical result. The comparison between the ACCM and theoretical first-order SSA model (SSA-1) data[19] at an incident angle of 50° illustrates that the ACCM works well in the specular directions and other nonspecular region, except for a little low agreement in the transition region between the specular and nonspecular region. However, the difference remains within acceptable range.

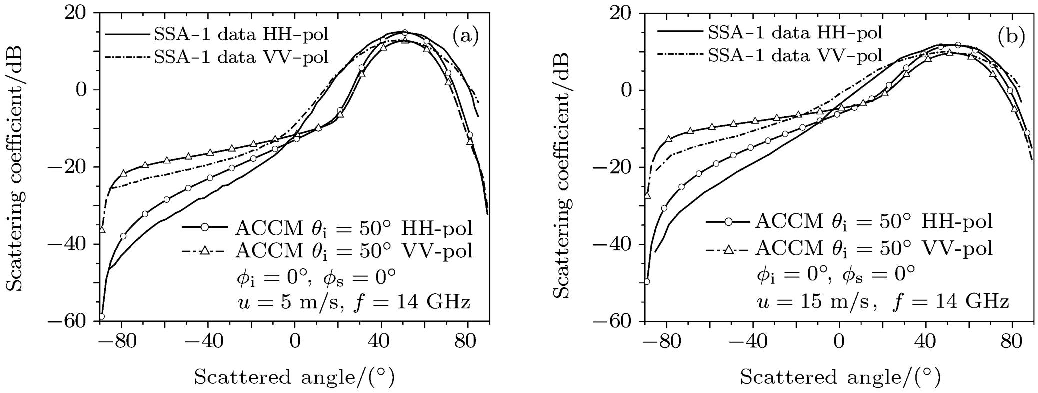

Fig. 5. Comparison of ACCM and SSA-1 data for angular distribution of the co-polarised bistatic scattering coefficient with incident angle $\theta_i = 50°$, $f = 14$ GHz: (a) $u = 5$ m/s; (b) $u = 15$ m/s.

4. Conclusion

In this paper, the electromagnetic scattering from two-dimensional rough sea surfaces has been investigated by using the ACCM. This new model is based on the local configuration angle division to select the corresponding method (KA or SPM) for electromagnetic scattering calculation. The dependence of the angular distribution of the scattering coefficient from rough sea surface on the wind speed, polarisation, as well as wind direction are analysed. The comparisons show good agreement between the ACCM and the experimental data and the theoretical results. Thus, the verification of the effectiveness and feasibility of the ACCM is attained.

References

[1] Liu Y, Wei E B, Hong J L and Ge Y 2006 *Chin. Phys.* **15** 2175

[2] Hu B J, Edward Yung K N, Zhang J and Serge T 2005 *Chin. Phys.* **14** 2305

[3] Li Y L, Huang J Y, Wang M J and Zhang J T 2008 *Chin. Phys.* B **17** 3394

[4] Chen G B, Wang H N, Yao J J and Han Z Y 2009 *Acta Phys. Sin.* **58** 3848 (in Chinese)

[5] Ye H X and Jin Y Q 2008 *Acta Phys. Sin.* **57** 839 (in Chinese)

[6] Elfouhaily T and Guerin C A 2004 *Waves in Random Media* **14** 1

[7] Valenzuela G R 1978 *Bound.-Layer Meteor.* **13** 61

[8] Winebrenner D P and Ishimaru A 1985 *J. Opt. Soc. Am.* **2** 2285

[9] Wright J W 1968 *IEEE Trans. Antennas Propag.* **16** 217

[10] Voronovich A G 1994 *Waves in Random Media* **4** 337

[11] Arnold-Bos A, Khenchaf A and Martin A 2007 *IEEE Trans. Geosci. Remote Sens.* **45** 3372

[12] Ulaby F T, Moore R K and Fung A K 1982 *Microwave Remote Sensing: Active and Passive* Vol. 2 (London: Addison-Wesley) p922

[13] Cox C and Munk W 1954 *J. Opt. Soc. Am.* A **44** 838

[14] Fung A K and Lee K K 1982 *IEEE J. Ocean Eng.* **OE-7** 166

[15] Khenchaf A and Airiau O 2000 *IEICE Trans. Electronics* **E83-C** 1827

[16] Wentz F J, Peteherich S and Thomas L A 1984 *J. Geophys. Res.* **89** 3689

[17] Voronovich A G and Zavorotni V U 2001 *Waves in Random Media* **11** 247

[18] Schroeder L C, Schaffner P R, Mitchell J L and Jones W L 1985 *IEEE J. Ocean Eng.* **OE-10** 346

[19] Awada A, Ayari M Y, Khenchaf A and Coatanhay A 2006 *Waves in Random Media* **16** 383